

Dynamics in a two-leg spin ladder with a four-spin cyclic interaction

Satoshi Nishimoto

Leibniz-Institut für Festkörper- und Werkstoffforschung Dresden, D-01171 Dresden, Germany

Mitsuhiro Arikawa

Institute of Physics, University of Tsukuba, 1-1-1 Tennodai, Tsukuba Ibaraki 305-8571, Japan

(Received 12 November 2008; revised manuscript received 6 February 2009; published 27 March 2009)

We study the two-leg Heisenberg ladder with four-spin cyclic interaction using the (dynamical) density-matrix renormalization-group method. We demonstrate the dependence of the low-lying excitations in the spin wave, staggered dimer order, and scalar-chirality order structure factors on the four-spin cyclic interaction. We find that the cyclic interaction enhances spin-spin correlations with wave vector around momentum $(q_x, q_y) = (\frac{\pi}{2}, 0)$. Also, the presence of long-range order in the staggered dimer and scalar-chirality phases is confirmed by a δ -function peak contribution of the structure factors at energy $\omega=0$.

DOI: 10.1103/PhysRevB.79.113106

PACS number(s): 75.10.Jm, 75.30.Kz, 75.40.Gb, 75.40.Mg

For many years, it had been generally believed that the magnetic properties of undoped high- T_c materials can be well described by the two-dimensional (2D) Heisenberg model with nearest-neighbor exchange interaction J . However, the four-spin cyclic interaction K has been increasingly recognized as a non-negligible correction to the Heisenberg model. The cyclic interaction comes from the fourth-order processes in the strong-coupling limit of the single-band Hubbard model at half filling.¹ The importance of this interaction was initially proposed in the 2D solid ³He, which has the hard-core correlations between spin- $\frac{1}{2}$ fermions.²

In fact, a substantial value $K=0.24 J$ was proposed for 2D copper oxide La_2CuO_4 by an accurate fit of the magnon dispersion.³ A close value was also suggested by an analysis of the Raman-scattering data.⁴ Such magnitude of the four-spin cyclic interaction must have a considerable influence at least quantitatively on the low-energy spin physics. Similar situations have been reported for several two-leg spin-ladder systems:⁵ the exchange interactions were estimated as $J_{\parallel} = J_{\perp} = 110$ meV and $K = 16.5$ meV for $\text{La}_6\text{Ca}_8\text{Cu}_{24}\text{O}_{41}$ (Ref. 6); $J_{\parallel} = 186$ meV, $J_{\perp} = 124$ meV, and $K = 31$ meV for $\text{La}_4\text{Sr}_{10}\text{Cu}_{24}\text{O}_{41}$ (Ref. 7); $J_{\parallel} = 165$ meV, $J_{\perp} = 150$ meV, and $K = 15$ meV for SrCu_2O_3 (Ref. 8), where J_{\parallel} and J_{\perp} are exchange interactions in the leg and rung directions, respectively.

Motivated by those observations, the ground-state properties of the two-leg spin- $\frac{1}{2}$ Heisenberg ladder with the four-spin cyclic interaction have been intensively studied.^{7,9-13} Also, the effect of magnetic field on the ground state has been investigated.¹⁴⁻¹⁶ Furthermore, the spectral features of the spin structure factor have been examined by the exact diagonalization, perturbation-theory, and density-matrix renormalization-group (DMRG) methods.¹⁷⁻²⁰ The spin dynamics for small-cyclic interactions is thus well understood, but the dynamical properties for other correlations and/or relatively large cyclic interactions are still open. In this Brief Report, we study the dynamical structure factors of staggered dimer order, scalar-chirality order, and spin waves for a wide range of the four-spin cyclic interaction to give a deeper insight into our knowledge of the low-lying excitations, using the dynamical DMRG (DDMRG) method.²¹

The Hamiltonian of the two-leg spin- $\frac{1}{2}$ Heisenberg ladder with the four-spin cyclic interaction is given by

$$H = J_{\parallel} \sum_{x,y} \vec{S}_{x,y} \cdot \vec{S}_{x+1,y} + J_{\perp} \sum_x \vec{S}_{x,1} \cdot \vec{S}_{x,2} + K \sum_x (P_x + P_x^{-1}), \quad (1)$$

with the cyclic permutation operator

$$\begin{aligned} P_x + P_x^{-1} = & \vec{S}_{x,1} \cdot \vec{S}_{x,2} + \vec{S}_{x+1,1} \cdot \vec{S}_{x+1,2} + \vec{S}_{x,1} \cdot \vec{S}_{x+1,1} + \vec{S}_{x,2} \cdot \vec{S}_{x+1,2} \\ & + \vec{S}_{x,1} \cdot \vec{S}_{x+1,2} + \vec{S}_{x,2} \cdot \vec{S}_{x+1,1} + 4(\vec{S}_{x,1} \cdot \vec{S}_{x,2}) \\ & \times (\vec{S}_{x+1,1} \cdot \vec{S}_{x+1,2}) + 4(\vec{S}_{x,1} \cdot \vec{S}_{x+1,1})(\vec{S}_{x,2} \cdot \vec{S}_{x+1,2}) \\ & - 4(\vec{S}_{x,1} \cdot \vec{S}_{x+1,2})(\vec{S}_{x,2} \cdot \vec{S}_{x+1,1}), \end{aligned} \quad (2)$$

where $\vec{S}_{x,y}$ is a spin- $\frac{1}{2}$ operator at a site (x, y) (see Fig. 1). For simplicity, we focus on the case of $J_{\parallel} = J_{\perp} = J$ and take $J=1$ as the unit of energy hereafter. The ground-state phase diagram was obtained in Ref. 10 as follows. The system has a rung-singlet phase for $-3.33 \leq K \leq 0.23$, a staggered dimer long-range-order (LRO) phase for $0.23 \leq K \leq 0.5$, a scalar-chirality LRO phase for $0.5 \leq K \leq 2.8$, a dominant vector chirality phase for $2.8 \leq K$, and a ferromagnetic phase for $K \leq -3.33$.

Let us define the dynamical structure factor as

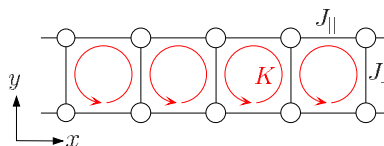


FIG. 1. (Color online) Lattice structure of the two-leg Heisenberg ladder. J_{\parallel} (J_{\perp}) is the exchange interaction in the leg (rung) direction and K is the four-spin cyclic interaction. The x - (y -) axis is defined as the leg (rung) direction.

$$A(\vec{q}, \omega) = \sum_{\nu} \langle \psi_0 | \hat{O}_{-\vec{q}} | \psi_{\nu} \rangle \langle \psi_{\nu} | \hat{O}_{\vec{q}} | \psi_0 \rangle \times \delta(\omega - E_{\nu} + E_0), \quad (3)$$

where $|\psi_{\nu}\rangle$ is the ν th eigenstate with the eigenenergy E_{ν} and $\hat{O}_{\vec{q}}$ is the Fourier transformation of the quantity-dependent operator $\hat{O}_{\vec{r}}$. The δ function is replaced by a Lorentzian with width η in our numerical calculations. We now study the following three kinds of the dynamical structure factor corresponding to three phases at $-3.3 \leq K \leq 2.8$. The first is spin structure factor $S(\vec{q}, \omega)$ with the operator

$$\hat{O}_{\vec{r}} = S_{x,y}^z, \quad (4)$$

where $S_{x,y}^z$ is the z component of the total spin, the second is dimer-order structure factor $D(\vec{q}, \omega)$ with

$$\hat{O}_{\vec{r}} = \vec{S}_{x-1,y} \cdot \vec{S}_{x,y} - \vec{S}_{x,y} \cdot \vec{S}_{x+1,y}, \quad (5)$$

and the third is scalar-chirality structure factor $C(\vec{q}, \omega)$ with

$$\hat{O}_{\vec{r}} = \vec{S}_{x,1} \cdot (\vec{S}_{x+1,1} \times \vec{S}_{x+1,2}). \quad (6)$$

By integrating Eq. (3), we can easily obtain the static structure factor

$$A(\vec{q}) = \langle \psi_0 | \hat{O}_{-\vec{q}} \hat{O}_{\vec{q}} | \psi_0 \rangle. \quad (7)$$

We employ the DDMRG method²¹ which is an extension of the standard DMRG method.²² It has been developed for calculating dynamical correlation functions at zero temperature in quantum lattice models. This method has been successfully applied to the one-dimensional Heisenberg model.²³ We now calculate the dynamical structure factor (3) with applying the periodic boundary conditions in the leg (x) direction. We fix the system length $L=32$ and $\eta=0.1$ if not otherwise stated. In the DDMRG calculation, a required CPU time increases rapidly with the number of the density-matrix eigenstates (m) so that we would like to keep it as few as possible; meanwhile, the DDMRG approach is based on a variational principle so that we have to prepare a ‘‘good trial function’’ of the ground state with the density-matrix eigenstates as much as possible. Therefore, we keep $m=600$ to obtain true ground state in the first ten DDMRG sweeps and keep $m=300$ to calculate the spectral functions. In this way, the maximum truncation error, i.e., the discarded weight, is about 3×10^{-4} , while the maximum error in the ground-state and low-lying excited-states energies is about 10^{-2} .

To begin with, we consider the spin structure factor. In Fig. 2, we show the DMRG results of the static and dynamical spin structure factors for the rung singlet ($K=0.1$), staggered dimer LRO ($K=0.4$), and scalar-chirality LRO ($K=0.7$) phases. The dispersion relations $\omega(\vec{q})$ are also plotted in the insets. The spectra for $q_y=0$ and π exhibit the two-triplon and one-triplon contributions, respectively. In the absence of the cyclic interaction, i.e., $K=0$,^{24,25} it is known that the spin dispersion has two minima at $q_x=0, \pi$ and a maximum at $q_x \sim 2\pi/3$ for $q_y=0$; whereas, two minima at $q_x=0, \pi$ and a maximum at $q_x \sim \pi/3$ for $q_y=\pi$. Those features have been confirmed to remain qualitatively unchanged at $K \leq 0.075$.¹⁹ For $K=0.1$, however, the minima at (q_x, q_y)

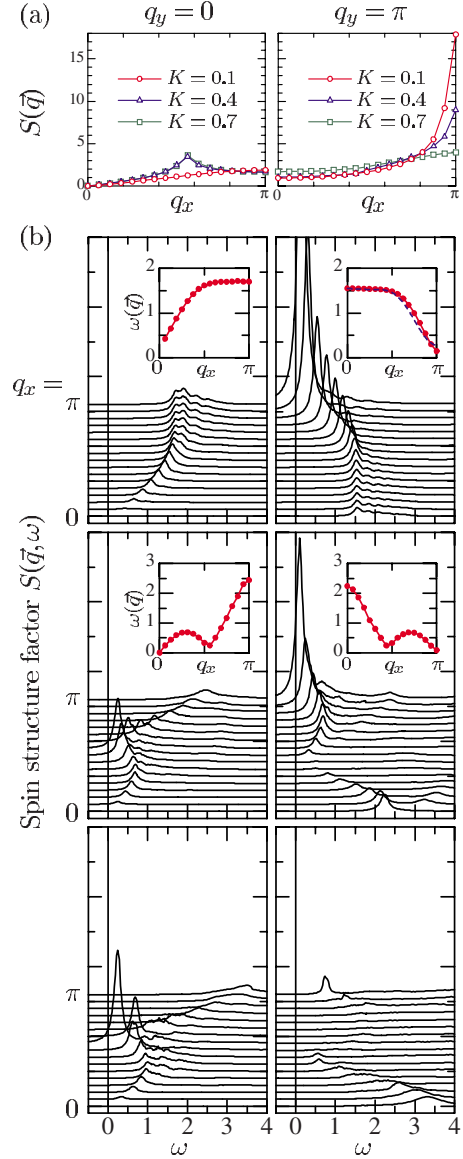


FIG. 2. (Color online) (a) Static spin structure factor. (b) Dynamical spin structure factor for $K=0.1$ (top), $K=0.4$ (middle), and $K=0.7$ (bottom). Left and right panels correspond to the results for $q_y=0$ and $q_y=\pi$, respectively. Insets: lower edge of the two-spinon continuum ($q_y=0$) and one-spinon dispersion ($q_y=\pi$). The dashed line denotes the perturbative result $\omega(q_x, q_y=\pi) = 1.186 + 0.558 \cos(q_x) - 0.271 \cos(2q_x) + 0.071 \cos(3q_x)$.

$=(\pi, 0), (0, \pi)$ are no longer visible [see the insets of the top panels in Fig. 2(b)], i.e., the dispersions are nearly flat around $(q_x, q_y) \sim (\pi, 0), (0, \pi)$. The one-triplon excitation ($q_y=\pi$) is in good agreement with the perturbative result.¹⁷ This is also consistent with other numerical study.¹⁸

When the cyclic interaction is further increased to $K=0.4$, we can see a drastic change in the spectra for both $q_y=0$ and π : especially, an enhancement of peaks around $(q_x, q_y) = (\frac{\pi}{2}, 0)$ and a reduction in peaks around $(q_x, q_y) = (\pi, \pi)$ are derived. It is because the cyclic interaction leads to a repulsive interaction between neighboring rung triplets. In addition, a node emerges at $q_x = \frac{\pi}{2}$ for both q_y values and a relation $\omega(q_x, q_y=0) = \omega(\pi - q_x, q_y=\pi)$ appears to be satis-

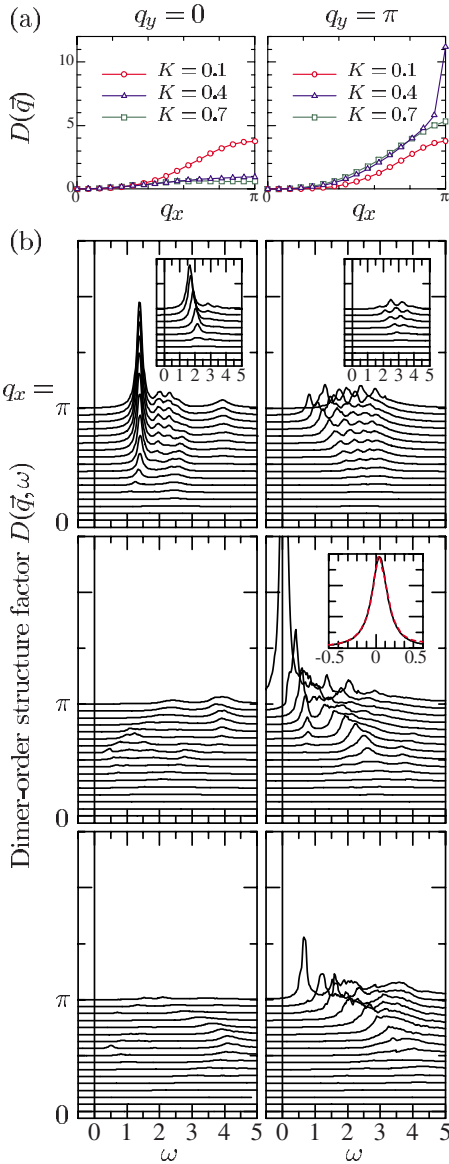


FIG. 3. (Color online) (a) Static dimer-order structure factor. (b) Dynamical dimer-order structure factors for $K=0.1$ (top), $K=0.4$ (middle), and $K=0.7$ (bottom). Left and right panels correspond to the results for $q_y=0$ and $q_y=\pi$, respectively. Insets of the top panels: $D(\vec{q}, \omega)$ for $K=0$ with $L=16$ and $\eta=0.2$. Inset of the middle panel: a Lorentzian fit of the peak at $(q_x, q_y)=(\pi, \pi)$ and $\omega \sim 0$ with $\eta=0.1$.

fied. They would indicate a twofold-degenerate ground state with a broken translational symmetry, which is consistent with the staggered dimer-order state. For $K=0.7$, the peaks around $(q_x, q_y)=(\frac{\pi}{2}, 0)$ are still more enhanced, whereas, the low-energy spectral features for $q_y=\pi$ seem to be much reduced. Actually, the one-triplon contribution is shunted off to the high-energy excitations since the static structure factor for $q_y=\pi$ is not much suppressed. In short, from the standpoint of spin-spin correlation, the four-spin cyclic interaction may work for enhancing a spin-density wave with wave vector $(q_x, q_y)=(\frac{\pi}{2}, 0)$ and for reducing the antiferromagnetic correlation $S(\pi, \pi)$ [see Fig. 2(a)].

Next, we turn to the dimer-order structure factor. Figure 3

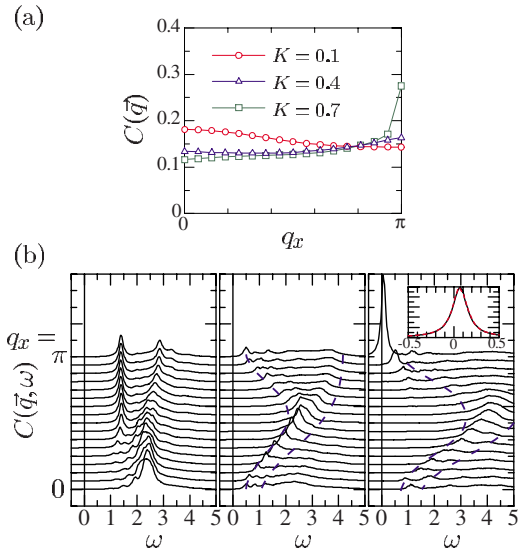


FIG. 4. (Color online) (a) Static scalar-chirality structure factor. (b) Dynamical scalar-chirality structure factors for $K=0.1$ (left), $K=0.4$ (center), and $K=0.7$ (right). Inset of the bottom panel: a Lorentzian fit of the peak at $q_x=\pi$ and $\omega \sim 0$ with $\eta=0.1$. The dashed lines denote the lower and upper edges of the continuum.

shows the DMRG results of the static and dynamical dimer-order structure factors for $K=0.1, 0.4$, and 0.7 . For comparison, the results of $D(\vec{q}, \omega)$ for $K=0$ are shown in the insets of the top panels of Fig. 3(b). In the rung-singlet phase, the ground state is approximately expressed as the product of local rung singlets with gap $\Delta \sim \mathcal{O}(J_\perp)$. The lowest excitation comes from the formation of a leg singlet with coupling energy $\sim \frac{J_\parallel}{2}$ as well as the collapse of two rung singlets. For $K=0$, therefore, undispersive sharp peaks appear around $\omega = \mathcal{O}(2\Delta - \frac{J_\parallel}{2}) \sim 1.5$ for $q_y=0$; whereas, the spectra for $q_y=\pi$ consist of broad continua at $\omega > \mathcal{O}(2\Delta - J_\parallel)$.

When small cyclic interaction ($K=0.1$) is introduced, we can see a strong influence on the continua around $(q_x, q_y)=(\pi, \pi)$, i.e., they are significantly shifted toward lower energies. It implies that the gap Δ is reduced rapidly as K increases. For $K=0.4$, the continua are further drastically changed: a pronounced peak appears at $(q_x, q_y)=(\pi, \pi)$ and $\omega \sim 0$; also, most of the spectral weight concentrates around the peak. On the other hand, the spectral weights for $q_y=0$ are totally suppressed. The pronounced peak is well fitted by a Lorentzian with $\eta=0.1$, as shown in the inset in the middle panel of Fig. 3(b). In other words, the spectrum for $(q_x, q_y)=(\pi, \pi)$ may consist of a δ -function peak at $\omega=0$ and a gapfull continuum. They would be a signature of long-range-staggered dimer order. For $K=0.7$, the spectral weights around $(q_x, q_y)=(\pi, \pi)$ are much reduced and a gap opens. It means that the staggered dimer order is no longer dominant in the ground state. Nevertheless, the spectral weights around $(q_x, q_y)=(\pi, \pi)$ are still significant, as seen in Fig. 3(a), so that the dimer-order correlation could just be changed from long-range order to short-range order. It is consistent with the fact that the staggered dimer-order parameter is finite even in the scalar-chirality LRO phase.¹⁰

Finally, we look at the scalar-chirality structure factor. The DMRG results of the static and dynamical scalar-

chirality structure factors for $K=0.1$, $K=0.4$, $K=0.7$ are shown in Fig. 4. For $K=0.1$, the lowest excitations are described by (almost) undispersive peaks around $\omega \sim \mathcal{O}(2\Delta - \frac{J_{\parallel}}{2})$ in analogy with the dimer-order structure factor. For $K=0.4$, the spectra form a continuum bounded by the branches $\omega(q_x) \sim A \sin(q_x)$ and $\omega(q_x) \sim 2A \sin(q_x/2)$, except that a gap opens at $q_x=0$ and π . The existence of the gap implies that the scalar-chirality order still belongs to an excited state. If we assume a complete staggered dimer order, i.e., the ground state is the product of local dimer singlets, the scalar-chirality operator (6) may be effectively reduced as $\vec{S}_{x,1} \cdot (\vec{S}_{x+1,1} \times \vec{S}_{x+1,2}) |\psi_0\rangle \approx (\vec{S}_{x,1}/2) |\psi_0\rangle$. Thus, the dispersions are similar to those of the spin structure factor in the one-dimensional spin-Peierls Heisenberg model.^{26,27} For $K=0.7$, we can see the closing of the gap and, moreover, the appearance of a dominant peak at $q_x=\pi$ and $\omega \sim 0$. This peak is well fitted by a Lorentzian with $\eta=0.1$, as shown in the inset of the right panel in Fig. 4(b). Hence, the spectrum for $q_x=\pi$ is composed of a δ -function peak at $\omega=0$ and a gapfull continuum, as is $D(\vec{q}, \omega)$ in the staggered dimer LRO phase.

It must indicate the presence of the scalar-chirality LRO.

In summary, we study the two-leg Heisenberg ladder with the cyclic four-spin interaction. The static and dynamical structure factors for the spin waves, staggered dimer order, and the scalar-chirality order parameters are calculated with the DDMRG method. We find that the spin-spin correlation with wave vector $(q_x, q_y) = (\frac{\pi}{2}, 0)$ is enhanced by the cyclic interaction. We also confirm the presence of long-range order in the staggered dimer and scalar-chirality phases by a δ -function peak contribution of the structure factor at $\omega=0$.

We thank M. Nakamura, S. Suga, T. Tohyama, T. Hikihara, T. Momoi, I. Maruyama, S. Tanaya, and Y. Hatsugai for useful discussions. This work has been supported in part by the University of Tsukuba Research Initiative and Grants-in-Aid for Scientific Research, from JSPS under Grant No. 20654034, from MEXT under Grants No. 220029004 (Physics of New Quantum Phases in Superclean Materials), and under No. 20046002 (Novel States of Matter Induced by Frustration) on Priority Areas for M.A.

-
- ¹M. Takahashi, J. Phys. C **10**, 1289 (1977).
²M. Roger, J. H. Hetherington, and J. M. Delrieu, Rev. Mod. Phys. **55**, 1 (1983).
³A. A. Katanin and A. P. Kampf, Phys. Rev. B **66**, 100403(R) (2002).
⁴Y. Honda, Y. Kuramoto, and T. Watanabe, Phys. Rev. B **47**, 11329 (1993).
⁵K. P. Schmidt, A. Gössling, U. Kuhlmann, C. Thomsen, A. Löffert, C. Gross, and W. Assmus, Phys. Rev. B **72**, 094419 (2005).
⁶M. Matsuda, K. Katsumata, R. S. Eccleston, S. Brehmer, and H.-J. Mikeska, Phys. Rev. B **62**, 8903 (2000).
⁷S. Notbohm, P. Ribeiro, B. Lake, D. A. Tennant, K. P. Schmidt, G. S. Uhrig, C. Hess, R. Klingeler, G. Behr, B. Buchner, M. Reehuis, R. I. Bewley, C. D. Frost, P. Manuel, and R. S. Eccleston, Phys. Rev. Lett. **98**, 027403 (2007).
⁸Y. Mizuno, T. Tohyama, and S. Maekawa, J. Low Temp. Phys. **117**, 389 (1999).
⁹A. A. Nersesyan and A. M. Tsvelik, Phys. Rev. Lett. **78**, 3939 (1997).
¹⁰A. Läuchli, G. Schmid, and M. Troyer, Phys. Rev. B **67**, 100409(R) (2003).
¹¹T. Hikihara, T. Momoi, and X. Hu, Phys. Rev. Lett. **90**, 087204 (2003).
¹²K. P. Schmidt, H. Monien, and G. S. Uhrig, Phys. Rev. B **67**, 184413 (2003).
¹³K. Hijii, S. Qin, and K. Nomura, Phys. Rev. B **68**, 134403 (2003).
¹⁴A. Nakasu, K. Totsuka, Y. Hasegawa, K. Okamoto, and T. Sakai, J. Phys.: Condens. Matter **13**, 7421 (2001).
¹⁵T. Hikihara and S. Yamamoto, J. Phys. Soc. Jpn. **77**, 014709 (2008).
¹⁶M. Sato, Phys. Rev. B **76**, 054427 (2007).
¹⁷S. Brehmer, H.-J. Mikeska, M. Müller, N. Nagaosa, and S. Uchida, Phys. Rev. B **60**, 329 (1999).
¹⁸N. Haga and S. I. Suga, Phys. Rev. B **66**, 132415 (2002).
¹⁹T. S. Nunner, P. Brune, T. Kopp, M. Windt, and M. Grüninger, Phys. Rev. B **66**, 180404(R) (2002).
²⁰K. Inaba and S. Suga, Prog. Theor. Phys. Suppl. **159**, 128 (2005).
²¹E. Jeckelmann, Phys. Rev. B **66**, 045114 (2002).
²²S. R. White, Phys. Rev. Lett. **69**, 2863 (1992); Phys. Rev. B **48**, 10345 (1993).
²³S. Nishimoto and M. Arikawa, Int. J. Mod. Phys. B **21**, 2262 (2007).
²⁴T. Barnes, E. Dagotto, J. Riera, and E. S. Swanson, Phys. Rev. B **47**, 3196 (1993).
²⁵R. Eder, Phys. Rev. B **57**, 12832 (1998).
²⁶A. M. Tsvelik, Phys. Rev. B **45**, 486 (1992).
²⁷S. Haas and E. Dagotto, Phys. Rev. B **52**, R14396 (1995).